(2)

AFWAL-TR-87-3020

BEHAVIOR OF A VORTICITY-INFLUENCED ASYMMETRIC STRESS TENSOR IN FLUID FLOW

C. H. Berdahl
W. Z. Strang

Aerodynamic Methods Group
Aeromechanics Division

October 1986

Final Report for 1 July 1985 - 29 May 1986

FLIGHT DYNAMICS LABORATORY
AIR FORCE WRIGHT AERONAUTICAL LABORATORIES
AIR FORCE SYSTEMS COMMAND
WRIGHT-PATTERSON AIR FORCE BASE, OHIO 45433-6553

NOTICE

When Government drawings, specifications, or other data are used for any purpose other than in connection with a definitely related Government procurement operation, the United States Government thereby incurs no responsibility nor any obligation whatsoever; and the fact that the Government may have formulated, furnished, or in any way supplied the said drawings, specifications, or other data, is not to be regarded by implication or otherwise as in any manner licensing the holder or any other person or corporation, or conveying any rights or permission to manufacture, use, or sell any patented invention that may in any way be related thereto.

This report has been reviewed by the Public Affairs Office (PA) and is releasable to the National Technical information Service (NTIS). At NTIS, it will be available to the general public, including foreign nations.

This technical report has been reviewed and is approved for publication.

Carl H. Berdahl
CARL H. BERDAHL, Capt, USAF
PROJECT ENGINEER

William Strang
WILLIAM Z. STRANG, Capt, USAF
PROJECT ENGINEER

Bohdan G. Kunciw
BOHDAN G. KUNCIW, Major, USAF
Chief,
Aerodynamics and Airframe Branch

FOR THE COMMANDER

Donald A. Dreesbach
DONALD A. DREESBACH, Colonel, USAF
Chief, Aeromechanics Division

Copies of this report should not be returned unless return is required by security considerations, contractural obligations, or notice on a specific document.

UNCLASSIFIED
SECURITY CLASSIFICATION OF THIS PAGE

AD-A181 245

REPORT DOCUMENTATION PAGE

Form Approved OMB No. 0704-0188

1a. REPORT SECURITY CLASSIFICATION: UNCLASSIFIED	1b. RESTRICTIVE MARKINGS: N/A
2a. SECURITY CLASSIFICATION AUTHORITY	3. DISTRIBUTION/AVAILABILITY OF REPORT: Approved for public release; DISTRIBUTION UNLIMITED
2b. DECLASSIFICATION/DOWNGRADING SCHEDULE	
4. PERFORMING ORGANIZATION REPORT NUMBER(S): AFWAL-TR-87-3020	5. MONITORING ORGANIZATION REPORT NUMBER(S)
6a. NAME OF PERFORMING ORGANIZATION: Flight Dynamics Laboratory, Air Force Wright Aeronautical Laboratories; 6b. OFFICE SYMBOL (If applicable): AFWAL/FIMM	7a. NAME OF MONITORING ORGANIZATION
6c. ADDRESS (City, State, and ZIP Code): Wright-Patterson AFB OH 45433-6553	7b. ADDRESS (City, State, and ZIP Code)
8a. NAME OF FUNDING/SPONSORING ORGANIZATION: Flight Dynamics Laboratory, Air Force Wright Aeronautical Laboratories; 8b. OFFICE SYMBOL (If applicable): AFWAL/FIMM	9. PROCUREMENT INSTRUMENT IDENTIFICATION NUMBER
8c. ADDRESS (City, State, and ZIP Code): Wright-Patterson AFB OH 45433-6553	10. SOURCE OF FUNDING NUMBERS: PROGRAM ELEMENT NO. PE-62201F 2404; PROJECT NO 10; TASK NO A1; WORK UNIT ACCESSION NO.

11. TITLE (Include Security Classification)
BEHAVIOR OF A VORTICITY-INFLUENCED ASYMMETRIC STRESS TENSOR IN FLUID FLOW

12. PERSONAL AUTHOR(S)
C.H. Berdahl and W.Z. Strang

13a. TYPE OF REPORT	13b. TIME COVERED	14. DATE OF REPORT (Year, Month, Day)	15. PAGE COUNT
Final Report	FROM 1Jul85 TO 29May86	1986 October	65

16. SUPPLEMENTARY NOTATION

17. COSATI CODES			18. SUBJECT TERMS (Continue on reverse if necessary and identify by block number)
FIELD	GROUP	SUB-GROUP	Stress, Constitutive Relation, Turbulence
20	04		

19. ABSTRACT (Continue on reverse if necessary and identify by block number)

The Navier-Stokes momentum equations describe the general movement of a Newtonian fluid. In the classic derivation of these equations, an entity called the stress tensor is postulated to exist. The stress tensor is a mathematical convenience that allows macro-scale modeling of the momentum transfer between molecules in a fluid. Classic thought assumed that such a stress tensor would depend linearly on the first order velocity gradients about a point, gradients that can be decomposed into dilatation, deformation, and vorticity. Furthermore, classic thought allowed the stress to depend on dilatation and deformation but assumed no effect of vorticity on stress. Because the complete Navier-Stokes equations had not yielded to numerical solution until the last few years, it had been impractical to test the validity of assuming no influence of vorticity on stress. However, the arrival of powerful computers has now made their numerical solution possible. Consequently, an investigation was made into the relative behavior of the classic stress tensor as compared to a vorticity influenced stress tensor. In the current work, a vorticity-influenced stress tensor is derived. Behavior of its principal axes is examined. Within the context of a linearized one-

20. DISTRIBUTION/AVAILABILITY OF ABSTRACT	21. ABSTRACT SECURITY CLASSIFICATION
☒ UNCLASSIFIED/UNLIMITED ☐ SAME AS RPT ☐ DTIC USERS	UNCLASSIFIED

22a NAME OF RESPONSIBLE INDIVIDUAL	22b TELEPHONE (Include Area Code)	22c OFFICE SYMBOL
C.H. Berdahl	513-255-3761	AFWAL/FIMM

DD Form 1473, JUN 86 — Previous editions are obsolete. — SECURITY CLASSIFICATION OF THIS PAGE: UNCLASSIFIED

dimensional momentum equation, the asymmetric stress tensor is shown to display a forcing function behavior in phase space under some conditions. Classic heuristic arguments are discussed for assuming no influence of vorticity on stress. Lastly, the behavior of a two-dimensional, low speed free shear layer is computed as it transitions from laminar to turbulent flow under the influence of the Stokesian tensor and then the vorticity-influenced tensor. The MacCormack, two-dimensional, explicit, time accurate, compressible code as implemented by Shang is used for this study. Results show that the two vorticity fields differ by a maximum of about one percent in the vicinity of some vortical structures.

FOREWORD

This report describes an in-house effort to develop a better technique for calculating turbulent flow. It has potential long-range application in many USAF problems such as computing the mixing rate of jet engine exhaust with ambient air, computing the drag rise due to turbulent flow over the airframe, and computing turbulent mixing in jet engine burner sections. The work was done under work unit 240410A1 in the Aerodynamics Methods Group, Aerodynamics and Airframe Branch, Aeromechanics Division, Flight Dynamics Laboratory, Air Force Wright Aeronautical Laboratories, Wright-Patterson AFB, Ohio.

TABLE OF CONTENTS

LIST OF ILLUSTRATIONS

LIST OF SYMBOLS

B_{ijpq}	fourth order tensor relating stress to velocity gradients
c	speed, constant
D_{ik}	deformation tensor, $\frac{1}{2}(u_{i,k} + u_{k,i})$
$\frac{D}{Dt}$	material derivative $(\frac{\partial}{dt} + u_i\frac{\partial}{\partial x_i})$
g	complex forcing function $(g = g_r + ig_i)$
G_i	ith component of body force
i	$(-1)^{\frac{1}{2}}$
k	wavenumber
K	grid index
P	thermodynamic pressure
t	time
u_i	ith component of velocity
x_i	position in Cartesian coordinates
x_i'	position in a coordinate system transforming in time
δ_{ij}	Kronecker delta
γ	eigenvalue
κ	bulk viscosity
λ	second viscosity coefficient
μ	shear viscosity (first viscosity coefficient)
ρ	fluid density

ω_{ij}	vorticity tensor
Ω	magnitude of vorticity vector
ν	vortex viscosity (third viscosity coefficient)
σ_{ij}	stress tensor

Subscripts

∞	denotes free stream condition
i,j,k,p,q	tensor subscripts denoting direction (x_1, x_2, or x_3)

SECTION I

INTRODUCTION

For over 140 years, fluid mechanics has used the Navier-Stokes equations (1:297) to describe fluid movement. Yet, until the arrival of large computers in the last five to ten years, it had been impossible to solve the Navier-Stokes equations in their complete form. In the past, workers obtained analytic solutions to simpler equations that were simplifications of the complete Navier-Stokes equations. For example, a simplified form of the Navier-Stokes momentum equations known as the Prandtl boundary layer equations were derived by assuming incompressible, two-dimensional flow. The Prandtl equations (and a derivative, Blasius' equation) enjoyed tremendous success in predicting the characteristics of laminar boundary layers (2:142).

Now that computers permit solution of the complete Navier-Stokes equations, workers still seem to prefer other forms of the Navier-Stokes equations than the basic primitive variable (pressure and velocity) form. For example, researchers have often recast the equations in a vorticity formulation or assumed spatial periodicity of the solution in order to obtain a solution that predicted vortical structures, the building blocks of turbulent flow. The favoritism given vorticity formulations is particularly interesting considering the picture of

turbulence emerging from the laboratory. Experimental observation has shown the vital role vortical structures play in turbulence. Although much of the rich vortical structure of turbulent flow appears to be born from inviscid interaction between different regions of fluid, viscous effects play a role by creating unstable velocity gradients in some cases and attenuating velocity gradients in other cases (3).

Despite this involvement of vortical structures and viscous influences in turbulence, the standard constitutive relation for stress does not admit the influence of vorticity. This state of affairs exists even though vorticity is one of three basic isotropic motions about a point (the other two being deformation and dilatation, both used in the standard constitutive relation). Heuristic and specious arguments have been presented (2:50 and 4:143-144) to justify omitting vorticity from the constitutive relation. For example, one argument assumes the stress tensor to be symmetric and then proceeds from this to "prove" that vorticity can not contribute to stress. This argument assumes the result and then uses this to prove the result. It is logically incorrect. This heritage of omission seems to stem more from an assumption Stokes made in 1845 (1:289-290) rather than from any rigorous proof of the symmetry of the stress tensor. Stokes simply assumed that vorticity did not influence viscous stress.

This paper will show that, by retaining the effect of vorticity on stress, a stress tensor can be obtained that has

intuitively appealing predictions of stress and a "different" behavior in vortical flows or, more generally, in regions where shearing fluid is turning away from the higher speed fluid. In particular, the vorticity-influenced stress tensor is asymmetric, and, by diagonalizing this stress tensor, the principal stresses become complex in these regions. A simple one-dimensional linear analysis using this complex principal stress suggests a dispersive or phase shift effect in vortical regions. Computer "thought" experiments comparing the behavior of the present vorticity-influenced stress tensor and the classic Stokesian stress tensor show a small difference in fluid behavior in a low-speed free shear layer.

SECTION II

THEORY

1. CLASSIC DEVELOPMENT OF STRESS TENSOR

The logical starting point for the classic development of the stress tensor is Cauchy's equation of motion, equation (1).

$$\rho \frac{D\, u_i}{Dt} = \rho G_i + \sigma_{ki,k} \tag{1}$$

Equation (1) describes the change in momentum of a point in a fluid due to body and surface forces (stresses). The Einstein summation convention is used. The subscripts i, j, p, and q can each take on the values 1, 2, or 3. Commas in the subscripts such as $u_{p,q}$ denote differentiation (i.e. $\frac{\partial u_p}{\partial x_q}$). The left-hand side of (1) describes the acceleration of the fluid while the right-hand side of (1) describes the forces exerted on the fluid. $\frac{D}{Dt}$ is the material (sometimes called substantial) derivative, ρ is the fluid density, u_i is the ith velocity component, G_i is the component of a body force (e.g. gravity), and σ_{ki} is a component of the stress tensor. The component,

σ_{ki}, is a generic stress that must be defined with a constitutive relation appropriate for the fluid of interest. This paper will focus on the nature of σ_{ki}.

Stokes made two assumptions when he presented his theory of stresses caused by velocity gradients. "That the difference between the pressure on a plane in a given direction passing through any point P of a fluid in motion and the pressure which would exist in all directions about P if the fluid in its neighborhood were in a state of relative equilibrium depends only on the relative motion of the fluid immediately about P; and that the relative motion due to any motion of rotation may be eliminated without affecting the differences of the pressures above mentioned" (1:289-290). Stokes italicized these words to emphasize that they were assumptions only.

Stokes first assumption effectively says

$$\sigma_{ij} = B_{ijpq}\, u_{p,q} \tag{2}$$

where σ_{ij} is the stress tensor, B_{ijpq} is a fourth order tensor, and $u_{p,q}$ is the fluid velocity gradient tensor.

Equation 2 states that any possible first-order velocity gradient could affect any of the nine stresses in σ_{ij}. Unfortunately, B_{ijpq} has 81 components, so Stokes was very

interested in simplifying the situation in order to generate a more manageable constitutive relation. He was able to do this by assuming that the fluid "looks the same" (is isotropic) no matter which way one looks in the fluid. This requires that the components of B_{ijpq} do not change under rotation to a new coordinate system. With this requirement in hand, the 81 components reduce to three. The general fourth order tensor (5:34) that results from this isotropy assumption is

$$B_{ijpq} = \lambda\delta_{ij}\delta_{pq} + \mu(\delta_{ip}\delta_{jq} + \delta_{iq}\delta_{jp}) + \nu(\delta_{ip}\delta_{jq} - \delta_{iq}\delta_{jp}) \quad , \quad (3)$$

where δ is the Kronecker delta, λ is the second viscosity, μ is the shear (first) viscosity, and ν is the vortex (third) viscosity.

Equation (3) "contains" three basic movements about a point. They are dilatation, deformation, and vorticity. Figure 1 shows the correspondence.

$\lambda\delta_{ij}\delta_{pq}$ $\mu(\delta_{ip}\delta_{jq}+\delta_{iq}\delta_{jp})$ $\nu(\delta_{ip}\delta_{jq}-\delta_{iq}\delta_{jp})$

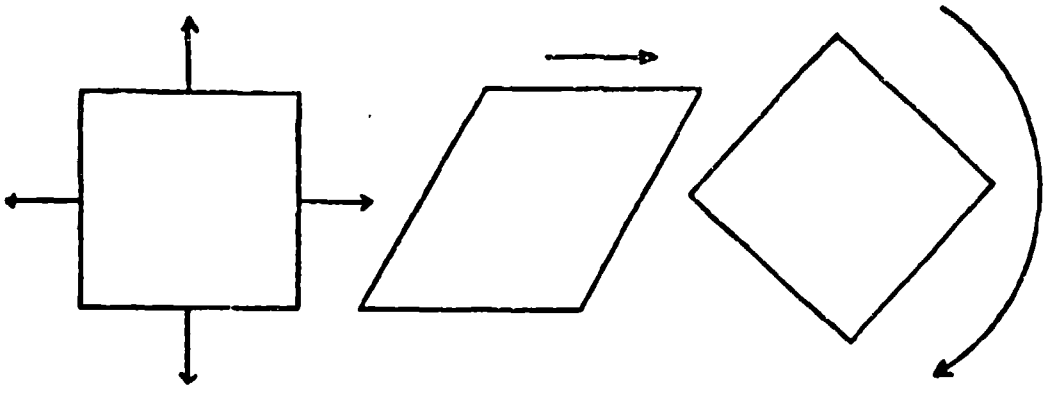

Dilatation Deformation Vorticity

Figure 1, Basic Movements from Isotropic Stress Relation

This correspondence might become a little clearer upon multiplying B_{ijpq} by $u_{p,q}$.

$$\sigma_{ij}=\begin{bmatrix} (\lambda+2\mu)u_{1,1}+ & (\mu+\nu)u_{1,2}+ & (\mu+\nu)u_{1,3}+ \\ \lambda(u_{2,2}+u_{3,3}) & (\mu-\nu)u_{2,1} & (\mu-\nu)u_{3,1} \\ (\mu-\nu)u_{1,2}+ & (\lambda+2\mu)u_{2,2}+ & (\mu+\nu)u_{2,3}+ \\ (\mu+\nu)u_{2,1} & \lambda(u_{1,1}+u_{3,3}) & (\mu-\nu)u_{3,2} \\ (\mu-\nu)u_{1,3}+ & (\mu-\nu)u_{2,3}+ & (\lambda+2\mu)u_{3,3}+ \\ (\mu+\nu)u_{3,1} & (\mu+\nu)u_{3,2} & \lambda(u_{1,1}+u_{2,2}) \end{bmatrix} \quad (4)$$

In relation (4), μ is multiplied by deformation-like groups $(u_{i,k}+ u_{k,i})$, λ is multiplied by dilatation, $u_{i,i}$, and ν is multiplied by vorticity-like groups, $(u_{i,k}- u_{k,i})$. Strictly speaking, deformation is $D_{ik}= \frac{1}{2} (u_{i,k}+ u_{k,i})$ and vorticity is $\omega_{ik}= \frac{1}{2} (u_{i,k}- u_{k,i})$. Stokes assumed away the effects of vorticity so he effectively set ν to be zero. (We shall later retain ν) At this point he had only two surviving constants: λ and μ. When he summed the diagonal components of (4) (the "trace"), he obtained $(3\lambda + 2\mu)u_{i,i}$ where the quantity $(3\lambda + 2\mu)$ is commonly called the bulk viscosity, κ (7:4). He reasoned that the average of the trace should simply be the local thermodynamic pressure, so he set $\lambda = -\frac{2}{3} \mu$ in order to have $\frac{1}{3} (3\lambda + 2\mu)u_{i,i}= 0$. In this way, he reduced the 81 coefficients to just one (μ).

In addition to these relative movement stresses, a fluid is also considered as having a pressure. Pressure can be added to the general stress tensor by adding in $-P\delta_{ij}$ so that relation (5) results.

$$\sigma_{ij}= -P\delta_{ij}+ \mu(u_{i,j}+ u_{j,i}) - \frac{2}{3} \mu \delta_{ij}u_{k,k} \qquad (5)$$

Consequently, in the absence of local fluid velocity gradients, the stress predicted is simply the pressure. Modern textbooks that use equation (5) as their constitutive relation for predicting stress in a fluid include one by White (6:69-70) and one by Schlichting. (2:64)

Not everyone subscribes to Stokes' hypothesis that $\lambda = -\frac{2}{3}\mu$, though. If we were to believe that the average of the trace should include not only the pressure, but also the stress due to dilatation, we could refrain from setting $\lambda = -\frac{2}{3}\mu$ and write

$$\sigma_{ij} = -P\delta_{ij} + \mu(u_{i,j} + u_{j,i}) + \lambda\delta_{ij}u_{k,k} \quad . \tag{6}$$

The average of the trace of this tensor would be $-P + \lambda u_{k,k}$. Thompson (7:20) is one modern textbook author who uses this form.

The value to be assigned λ has been vigorously debated for many years. Experiments in acoustical streaming and sound wave attenuation support the idea that λ is not negative at all but positive and, in some cases, larger than the shear viscosity, μ, by two orders of magnitude. (7:21) To complicate matters, λ appears to be frequency dependent. The experimental procedures themselves are controversial. See Karim and Rosenhead (8), Rosenhead (9), or Truesdell (10:228-231) for a review of the

basic issues. Modern-day computational fluid dynamicists appear to accept the idea that $\lambda = -\frac{2}{3}\mu$ without question. Use of $\lambda = -\frac{2}{3}\mu$ probably does not make any difference for most flows since the dilatation or compression rates are low. For acoustic motions and the interior of shock waves, though, the dilatative stress can be significant (7:21).

The arguments about the second viscosity coefficient aside, there remain a few observations about the Stokesian tensor that will be useful for later discussions in this paper. Because of the Stokesian assumption of $\nu = 0$, the resulting stress tensor is symmetric. Given this symmetry, linear algebra enables one to find an orientation for a small fluid cube that will cause all the shear stresses on the faces of the cube to disappear, leaving only normal stresses. This is really an eigenvalue problem where the normal stresses in the diagonalized stress tensor are called the principal stresses. For the symmetric tensor, these principal stresses have some intuitively attractive properties, namely, they are always real and mutually orthogonal. One unsatisfying result, though, is that the symmetric tensor predicts shear stresses on faces of a small fluid cube even with no shearing rate of strain parallel to that face. Figure 2 makes the point. Imagine flow over a flat plate. In laminar flow, the velocity gradient is primarily $u_{1,2}$. A shear stress should form on the top face (x_2 or the A

face), and the symmetric stress tensor predicts this. What is not at all clear is why a shear stress would form on the side face (x_1 or the B face), but this is what Stokes' symmetric form predicts.

Another unsatisfying consequence of the $\nu = 0$ assumption is that, although isotropy shows that there are three basic types of motion about a point (Figure 1), the $\nu = 0$ form ignores one of them, the vorticity. These objections will surface again later in the paper in comparing the behavior of a vorticity-influenced stress tensor with the Stokesian tensor.

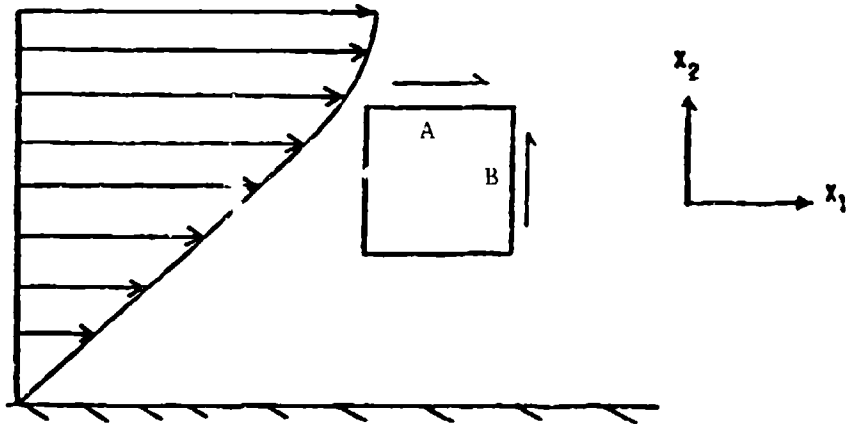

Figure 2, $\nu = 0$ Stress Square

Before leaving Stokes' form, though, here is its x_1 momentum equation for future reference. It is formed by substituting (6) into (1) and ignoring body forces.

$$\rho \frac{Du_1}{Dt} = P_{,1} + (\lambda u_{k,k})_{,1} + 2\mu u_{1,1,1} + \mu u_{1,2,2} + \mu u_{2,1,2} \qquad (7)$$

$$+ \mu u_{1,3,3} + \mu u_{3,1,3}$$

2. DEVIATION FROM CLASSIC THOUGHT: VORTICITY CONTRIBUTION TO STRESS

Let's return now to the role vorticity could play in viscous stress. For a long time, vorticity has seemed involved somehow with turbulence. A few examples illustrate this point. O. Reynolds, generally credited with conducting the first scientific study of turbulence, noted in 1883: "On viewing the tube by the light of an electric spark, the mass of colour resolved itself into a mass of more or less distinct curls, showing eddies..."(11: 942). Van Driest and Blumer (12) correlated a "vorticity Reynolds number" with laminar-turbulent transition results for a flat plate. Results were excellent, but White dismissed it by saying "Since the concept of a critical vorticity Reynolds number is obviously questionable and not related to any fundamental rigorous analysis, we can regard the van Driest-Blumer correlation simply as an excellent semiempiricism" (6:435).

Contemporary descriptions of turbulence also invoke the role of vorticity. Morkovin (3:0.01 - p1) observes: "the

continuously distributed vorticity in the base shear layer undergoes successive instabilities, i.e. transformations into increasingly more complex spatial and temporal patterns of vorticity concentrations." Dimotakis (13) has succinctly defined turbulence as "vorticity fluctuations."

Researchers trying to directly compute turbulence appear to prefer non-primitive variable formulations of the Navier-Stokes equations (e.g. vorticity-stream function). Fasel comments: "In reviewing literature on numerical simulations of viscous incompressible flows it is noticeable that formulations involving a vorticity-transport equation, rather than the primitive variable formulation, are preferred. The unpopularity of the u, v, p system is a result of numerable unsuccessful attempts in applying it to calculations of viscous incompressible flows" (14:9).

With all this attention focused on vorticity in order to understand turbulence, it's only reasonable to return to the constitutive relation Stokes developed for the Navier-Stokes equations and see how vorticity might be involved. We will deviate from Stokes' line of reasoning by allowing the vortex viscosity, ν, to survive the derivation of a constitutive relation. The first issue, on taking this course, is to choose a plausible value for ν.

One might choose ν to be the same magnitude as μ. In this case, according to relation $\mu = \nu$ or $\mu = -\nu$. This says that

vorticity, $\omega_{ij} = \frac{1}{2}(u_{i,j} - u_{j,i})$, causes stress of the same magnitude as deformation, $D_{ij} = \frac{1}{2}(u_{i,j} + u_{j,i})$. This seems a reasonable choice because both vorticity and deformation contain the same shearing gradients. What follows is a discussion of the implications of these two forms ($\mu = \nu$ and $\mu = -\nu$) and a comparison to Stokes' form ($\nu = 0$).

As Figure 1 shows, the stress tensor must consider the effects of dilatation, deformation, and vorticity to stay perfectly general in its isotropic form. The $\nu = \mu$ form of σ_{ij} appears an attractive choice because equating μ and ν says ν and μ behave in similar ways. Unfortunately, on replacing ν with μ in (4) and writing out the x_1 momentum equation, the $u_{1,2,2}$ and $u_{1,3,3}$ terms are seen to be missing.

$$\rho\frac{Du_1}{Dt} = -P_{,1} + (\lambda u_{k,k})_{,1} + 2\mu u_{1,1,1} + 2\mu u_{2,1,2} + 2\mu u_{3,1,3} \qquad (8)$$

The $u_{1,2,2}$ term is the term surviving from the classic Navier-Stokes equations when neglecting small terms to obtain the Prandtl equations for two-dimensional, laminar boundary layers. The Prandtl equations have been extremely successful in predicting characteristics of laminar boundary layers. In particular, the Blasius equation, a simplified form of Prandtl's equations, has convincingly predicted the laminar boundary layer

velocity profile (2:142). The absence of the $u_{1,2,2}$ term for the $\nu = \mu$ form is grounds for summarily dismissing it from further study.

That leaves the other possibility, that of $\nu = -\mu$. Some very interesting results stem from this case. By replacing ν with $-\mu$ in (4), a "$\mu = -\nu$ form" of the stress tensor results.

$$\sigma_{ij} = \begin{bmatrix} (\lambda + 2\mu)u_{1,1} + & & \\ \lambda(u_{2,2}+u_{3,3}) & 2\mu u_{2,1} & 2\mu u_{3,1} \\ & (\lambda + 2\mu)u_{2,2} + & \\ 2\mu u_{1,2} & \lambda(u_{1,1}+ u_{3,3}) & 2\mu u_{3,2} \\ & & (\lambda + 2\mu)u_{3,3} + \\ 2\mu u_{1,3} & 2\mu u_{2,3} & \lambda(u_{1,1}+ u_{2,2}) \end{bmatrix} \quad (9)$$

By substituting (9) into (1), the asymmetric stress tensor momentum equations can be written as following.

$$\rho \frac{Du_i}{Dt} = -P_{,i} + (\lambda u_{k,k})_{,i} + 2\mu u_{i,k,k} \quad (10)$$

An x_1 momentum equation can be obtained from equation 10 by setting i=1. Then, by expanding the $2\mu u_{i,k,k}$ term, the following equation results.

$$\rho \frac{Du_1}{Dt} = -P_{,1} + (\lambda u_{k,k})_{,1} + 2\mu u_{1,1,1} + 2\mu u_{1,2,2} + 2\mu u_{1,3,3} \qquad (11)$$

This $\mu = -\nu$ form of the x_1 momentum equation is somewhat different from the $\nu = 0$ form of the x_1 momentum equation (equation 7) although it has similarities. Equation 7 contains two more viscous terms than does equation 11. Also, the last two viscous terms in (11) have factors of two not present in the corresponding terms in (7).

These differences virtually vanish in the case of incompressible flow, though. By applying the incompressible continuity equation ($u_{i,i}=0$) to (7), the following equation results.

$$\rho \frac{Du_1}{Dt} = -P_{,1} + \mu u_{1,1,1} + \mu u_{1,2,2} + \mu u_{1,3,3} \qquad (12)$$

By applying the incompressibility assumption to (11), the following equation results.

$$\rho \frac{Du_1}{Dt} = -P_{,1} + 2\mu u_{1,1,1} + 2\mu u_{1,2,2} + 2\mu u_{1,3,3} \qquad (13)$$

As the reader can see, equation 13 has identically the same form as equation 12. The only difference is in the factors of two in the viscous terms in (13). For practical purposes, this is no difference at all because the shear viscosity, μ, is obtained experimentally with devices that assume the momentum equation looks like (12). In other words, the coefficient, μ, in (12) is an arbitrary coefficient just as is the coefficient, 2μ, in (13); the coefficients are simply assigned values based on experimental results.

Note that one can proceed further from (13) and obtain Prandtl's boundary layer equations through the usual arguments.

3. IMPLICATIONS OF THE $\mu = -\nu$ STRESS TENSOR

The $\mu = -\nu$ assumption has intuitive advantages over Stokes' $\nu = 0$ assumption. Consider the drawing of a small fluid square for the $\mu = -\nu$ form (Figure 3). The square is in a laminar boundary layer.

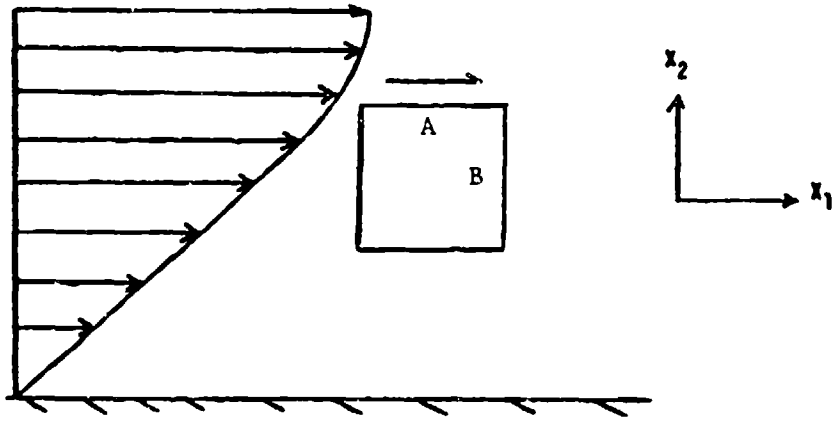

Figure 3, $\mu = -\nu$ Stress Square

This form predicts no stress on an adjacent face given that the only rate of strain gradient is out the x_2 face. This state of affairs appears to satisfy causality. Equation 11 says that viscous forces in the x_1 direction are simply due to the total diffusion of x_1 momentum through the faces of the cube. Alternatively, they describe how rapidly x_1 momentum arrives or leaves a small region of fluid. So, like heat or self diffusion of gases, the transport of molecular momentum in a given direction is simply proportional to the second spatial derivative of the momentum in that same direction. It is not simultaneously dependent on velocity gradients out of other

faces of a fluid stress cube as Stokes hypothesized when he assumed $\nu = 0$.

Another intuitive advantage of the $\mu = -\nu$ tensor is that it accounts for all three basic movements about a point (Figure 1), not just two of them as with the $\nu = 0$ form. The $\mu = -\nu$ form, then, would seem to give a more complete accounting of the viscous stress in the fluid as a result.

Although the stresses for the $\mu = -\nu$ stress tensor have this intuitively satisfying behavior, the $\mu = -\nu$ stress tensor raises some questions about the proper interpretation of the principal stresses. But, before elaborating on this, here is a little background about the principal stresses.

Stokes showed that the $\nu = 0$ stress tensor could be diagonalized to create only normal stresses by rotating a fluid cube to a particular orientation. See Figure 4.

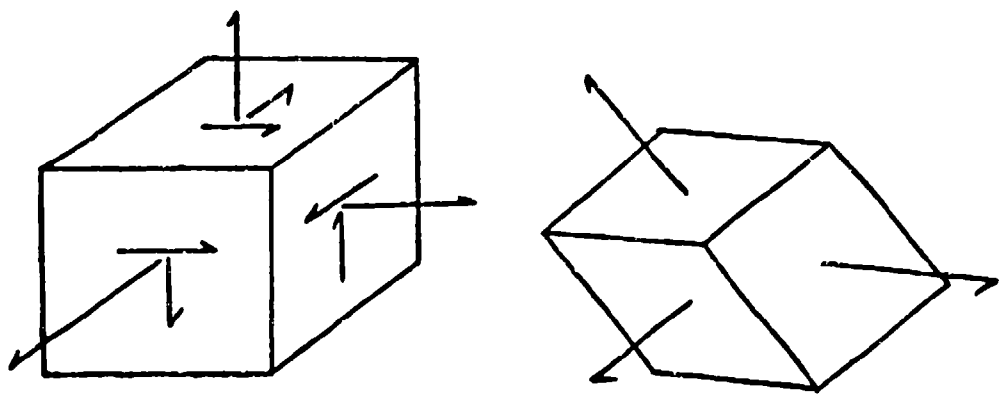

Figure 4, Normalizing a Stress Cube By Transforming

In a way, then, he envisioned viscous effects simply as pressures, and, in fact, Stokes used the word, "pressure," to describe viscous stresses. He seemed to be addressing the point of view of hydrodynamics, a point of view that recognized thermodynamic pressure but did not recognize viscous forces. Indeed, his interpretation of viscous effects as stresses (i.e. forces per unit area) seemed to stem from his hydrodynamic heritage.

With this interpretation of viscous effects as pressures in mind, note that one can also diagonalize the $\mu = -\nu$ stress tensor. However, under some conditions, the resulting principal stresses become complex, i.e. contain real and imaginary parts. This may be shown with the two-dimensional, incompressible form of the $\mu = -\nu$ stress tensor.

$$\sigma_{ij} = \begin{bmatrix} 2\mu u_{1,1} & 2\mu u_{2,1} \\ 2\mu u_{1,2} & 2\mu u_{2,2} \end{bmatrix} \tag{14}$$

By solving for the eigenvalues of (14), one can learn something about the behavior of the principal stresses. By factoring out the common quantity, 2μ, and introducing γ, the eigenvalues, the following results.

$$\sigma_{ij}=2\mu \begin{bmatrix} u_{1,1}-\gamma & u_{2,1} \\ u_{1,2} & u_{2,2}-\gamma \end{bmatrix} \tag{15}$$

By Cramer's rule for the determinant, we obtain the characteristic equation.

$$(u_{1,1}-\gamma)(u_{2,2}-\gamma) - u_{1,2}u_{2,1}=0 \tag{16}$$

Solving, we find the eigenvalues to be:

$$\gamma = \frac{1}{2}\left[-(u_{1,1}+u_{2,2}) \pm \left[(u_{1,1}+u_{2,2})^2 - 4(u_{1,1}u_{2,2}-u_{1,2}u_{2,1})\right]^{\frac{1}{2}}\right] . \tag{17}$$

The corresponding eigenvectors are

$$\begin{bmatrix} \dfrac{-u_{2,1}}{u_{1,1}-\gamma} \\ 1 \end{bmatrix} \quad \text{and} \quad \begin{bmatrix} \dfrac{\gamma - u_{2,2}}{u_{1,2}} \\ 1 \end{bmatrix} .$$

The incompressible flow assumption reduces (17) to:

$$\gamma = \pm(u_{1,2}\, u_{2,1} - u_{1,1}\, u_{2,2})^{\frac{1}{2}} \tag{18}$$

One can easily see that the eigenvectors corresponding to these eigenvalues will or will not have complex components depending on whether or not the eigenvalues are imaginary. Equation (18) shows that the eigenvalues will be imaginary if $u_{1,1}u_{2,2} > u_{1,2}u_{2,1}$. We call this condition the "phase shift criterion."

The complex nature of the principal stresses suggests that they could act like a complex forcing function in regions of the flow where the phase shift criterion was met. The imaginary component of the principal stress suggests a dispersive effect during which different wavelengths might be forced to move at different speeds. Unfortunately, the study of such an effect should be done in at least two dimensions for otherwise the principal stresses could not be complex. This fact complicates the analysis considerably. In three dimensions, the problem is much worse because many combinations of flow gradients could create complex principal stresses and the magnitude of the imaginary part varies with both the sign and magnitude of the velocity gradients.

Despite this intractable situation, one fact surfaces about complex principal stresses in two-dimensions. By inspection,

equation 18 says that the principal stresses will be complex whenever a shearing flow turns away from the higher speed flow (unless normal velocity gradients, $u_{1,1}$ and $u_{2,2}$ for the two-dimensional case, dominate). This would typically occur in a vortex. A detailed mapping of regions where the phase shift criterion is met in a two-dimensional free shear layer will appear later in the paper in the description of numerical experiments.

In addition to this descriptive approach to understanding the consequences of complex principal stresses, one could also study a one-dimensional linearized equation similar in some respects to the momentum equations but with a complex forcing function. Although much is lost in linearizing the partial differential equation, the linearized system still might offer some insight into how a complex forcing function would affect the fluid.

The one-dimensional, inviscid scalar convective equation serves as a starting point for such a study.

$$\frac{\partial u}{\partial t} + c\frac{\partial u}{\partial x} = 0 \qquad (19)$$

Here, u is velocity, t is time, c is the wave speed, and x is postion. Assume that $u = e^{\alpha t} e^{ikx}$ is the general solution to (19) where α is a complex number a + ib, t is the time, i is $(-1)^{\frac{1}{2}}$, k is a wavenumber, and x is the position. By differentiating the assumed solution and substituting into (19), the following solution is obtained.

$$u = e^{ik(x-ct)} \tag{20}$$

This solution says that all wavelengths convect at the same wave speed so that the starting u in x is simply shifted a distance ct in time t.

Now let's change (19) by modeling the effect of complex principal stress. It's already apparent that at least two dimensions are required to have principal stresses that are complex, but we suggest as a crude model the following equation.

$$\frac{\partial u}{\partial t} + c \frac{\partial u}{\partial x} = (g_r + i g_i) \frac{\partial^2 u}{\partial x^2} \tag{21}$$

Equation 21 is the same as the one-dimensional scalar convective equation (19) with the exception of the appearance of a viscous

type term with a complex coefficient. In general, $g_r + ig_i$ will vary with time, but it is held constant for the current problem to simplify the analysis.

Assuming the general solution of (21) to be $u = e^{\alpha t}e^{ikx}$, differentiating this assumed solution and substituting the derivatives back into (21) results in the following solution.

$$u = e^{-k^2 g_r t} e^{i[k(x-ct-kg_i t)]} \tag{22}$$

To the extent that equation (21) captures some of the dynamics of the full, multi-dimensional partial differential equations, (22) suggests that an imaginary component in the principal stress would have a dispersive or phase shift effect. This is so because of the appearance of an additional term $(-kg_i t)$ subtracted from x-ct. For comparison, see equation (20).

In summary, here are the consequences of the $\mu = -\nu$ form of the stress tensor. By accounting for all three types of basic motion about a point, we find an intuitively appealing diffusion of linear momentum through the different faces of a small fluid cube. Stresses arise on a given face of a cube only if there exists a shearing velocity gradient when viewed out of that face. Upon diagonalizing this stress tensor, the principal stresses are shown to be complex only under a condition called the phase shift criterion. This complex behavior arises when

the velocity gradients turn a shearing flow away from the higher speed flow such as would occur in a vortex.

4. OBJECTIONS TO ASYMMETRIC ($\mu = -\nu$) STRESS TENSOR DISCUSSED

There probably would be objections to the idea of an asymmetric stress tensor although it accounts, as shown, for all three basic types of motion about a point and not just the two proposed by Stokes. One objection is the argument that material indifference is violated. Material indifference heuristically requires that the stresses predicted in the fluid do not depend on the observer's motion (5:191). In the case of the $\mu = -\nu$ stress tensor, observer rotation would impress a kind of solid body rotation on the fluid with the vorticity contributed by the observer's rotation everywhere equal to half the rate of the observer's rotation. Since the $\mu = -\nu$ stress tensor predicts that vorticity will contribute to stress, a rotating coordinate system (rotating observer) will create stress under this model. This problem would disappear by specifying a non-rotating coordinate system, but this isn't really necessary as will be shown later.

If one considers coordinate system rotation simply as a time rate of change of a coordinate system, some inconsistencies in the material indifference argument appear. Take for example the dilating coordinate system that transforms according to the equation $x_i' = cx_i$ where c is a constant speed If the x_i

coordinate system had a velocity field of $u_i = cx_i$, then an observer in the x_i system would see a dilatation of 3c, while the observer in the x_i' system would see a dilatation of zero. Following the material indifference argument, one must exclude dilatation from the constitutive relation because the stress due to dilatation would not be the same for all observers just as was the case with the rotating coordinate system.

Similarly, a coordinate system that transforms according to a simple shearing motion, say $x_1' = cx_2$, with a velocity field in the unprimed system of $u_1 = cx_2$ would have an observer in the x_i coordinate system seeing the shearing motion, but an observer in the x_i' system would not see it. This shearing would give a deformation, D_{12}, of $\frac{1}{2}$ c. Again, the material indifference argument would find that the stress seen by the two observers would not be the same because of the different values of deformation seen in the two systems so, as a result, deformation would have to be excluded from the constitutive relation.

This line of thought, then, would lead to the conclusion that all three basic types of isotropic motion (vorticity, dilatation, and deformation) would not be permitted in predicting fluid stress. Fortunately, there may be an escape from this dilemma. All the distorting coordinate systems mentioned above have a common behavior. They all have a homogeneous motion contribution in the coordinate system. In

the case of rotation, the system has a spin rate everywhere the same. In the case of the dilating coordinate system, the system has a dilatation rate everywhere the same. In the case of the shearing coordinate system, the system has a shear rate everywhere the same. Since viscous effects are thought to manifest themselves as surface stresses, the divergence theorem says that only gradients of these stresses will create a net force on a region of fluid. In the three coordinate systems just described, the gradients of motion (due to coordinate system distortion rates) would all be zero because the system motion is everywhere the same. Consequently, a better way to approach the issue of material indifference when building a constitutive relation for fluid stress would be to admit "motions" due to time rate of change of a coordinate system as long as the contribution was the same (i.e. homogeneous) throughout the system.

Another objection to an asymmetric stress tensor is the idea that a small fluid cube under asymmetric stress would spin infinitely fast. Supposedly, the thinking goes, as the cube becomes smaller, the surface area decreases as the length squared while the volume (and the mass) decreases as the length cubed. Therefore, the shear stress has progressively more influence and, in the limit, the cube would spin infinitely fast.

The fallacy in this argument is in the assumption that the fluid is a continuum. This assumption is false. As the

hypothetical cube becomes smaller and smaller, eventually, individual molecules are recognized colliding in the cube and leaving or entering the cube, contributing or acquiring linear momentum from the fluid in the region. The continuum differential equations do not recognize these facts because they profess to be valid at each infinitesimal point with any point divisible into an arbitrarily smaller point. This is simply not true in a real fluid, yet the continuum line of thought induces one to visualize a small cube of continuum substance that will spin if torqued. Even if one begins to consider individual molecules, continuum thought may persist by making one believe that an asymmetric stress on a small "cube" of molecules would have to set all the molecules accelerating in spin to balance the torque applied. But even this viewpoint does not seem reasonable if there is no preferred form of collision between molecules in a region of shear that would set them spinning preferentially with a certain spin vector.

Another comment about continuum thinking is appropriate. Continuum theory prohibits two points in the continuum from mapping into one point or vice versa. Yet this is effectively just what is happening when molecules from two different regions of fluid diffuse into the same region. This is after all how diffusive transport of momentum and energy is possible. The viscous "stress" arises only by diffusion of individual molecules through the different faces of the arbitrarily defined cube. Hence, it seems unreasonable to apply a continuum

argument to justify what is a non-continuum phenomenon. There is no inherent ability to spin our hypothetical cube, because the cube merely consists of a box that happens to contain a few molecules just passing through and occasionally suffering a collision.

In addition to the above discussion, the reader may find the work by molecular dynamicists useful in considering the utility of material indifference. Molecular dynamicists directly simulate the kinematics of large numbers of molecules with computational techniques, and a summary of their misgivings about material indifference can be found in Evans and Hoover (15:259-260).

5. WHICH STRESS TENSOR IS BETTER?

Inevitably, the philosophical arguments used to justify one mathematical model over another are driven by the conclusion, in many cases heuristic, that one already has in mind. The real test comes when the models are compared with observations of nature. Unfortunately, many of the mathematical models, chiefly the non-linear ones, have defied solution until the arrival of large computers able to solve them in a discretized analog form. It now looks attractive to compare non-linear model predictions with nature by solving the non-linear systems on a computer.

One attractive possibility for such a comparison would be to use molecular dynamics. With a powerful enough computer,

large enough systems of molecules could be simulated that could perhaps answer the question of how best to relate the change in momentum of a region of fluid to mean velocity gradients. The reader is referred to Evans and Hoover (15) for information on progress in this area.

In the present work, however, the computer is used to solve the continuum equations and thereby compare the behavior of the two stress tensors. In this way, the computer can be considered as a "Gedankenversuch" (thought experiment) machine.

SECTION III

COMPUTER EXPERIMENTS

1. Problem Setup

This comparison between the stress tensors was done by computing a free shear layer using a two-dimensional, time-accurate, compressible Navier-Stokes code. This code served as a discrete analog to the two-dimensional Navier-Stokes partial differential equations. The only restriction beyond the two-dimensionality was that the second viscosity coefficient, λ, was set equal to zero for the experiments. This was done because the value to be assigned λ is controversial anyway, dilatative effects were thought to be small, and the real focus of the experiments was on the viscosity coefficients, μ and ν.

The momentum equations which were solved are presented below so as to avoid any confusion over just which momentum equations were used in the computer experiments. The x_1 and x_2 momentum equations containing the $\mu = -\nu$ stress tensor appear in equations 23 and 24, respectively.

$$\rho \frac{Du_1}{Dt} = -P_{,1} + \mu(u_{1,1,1} + u_{1,2,2}) \qquad (23)$$

$$\rho \frac{Du_2}{Dt} = -P_{,2} + \mu(u_{2,1,1} + u_{2,2,2}) \qquad (24)$$

Equations 23 and 24 may be derived from (13) by assuming two-dimensional flow and setting $\lambda = 0$. Although (23) and (24) contain the $\mu = -\nu$ assumption, μ and ν are both assigned half the value of the conventional shear viscosity. This is done for reasons explained in the text immediately following (13).

The $\nu = 0$ momentum equations used in the computer experiments appear in (25) and (26) for the x_1 and x_2 directions, respectively.

$$\rho \frac{Du_1}{Dt} = -P_{,1} + \mu(u_{1,1,1} + u_{1,2,2}) + \mu(u_{1,1,1} + u_{2,1,2}) \qquad (25)$$

$$\rho \frac{Du_2}{Dt} = -P_{,2} + \mu(u_{2,1,1} + u_{2,2,2}) + \mu(u_{2,2,2} + u_{1,2,1}) \qquad (26)$$

The reader may derive (25) and (26) from (6) and (1) by assuming two-dimensional flow and setting $\lambda = 0$.

A free shear layer computation was used for the computer experiments, because a free shear layer is a simple flow for which there is experimental data and such a computation reduced

numerical concerns over well-posed boundary conditions near the region of shear by keeping the boundaries of the computational domain away from the shear region (except near the upstream and downstream boundaries). This, of course, would not have been the case for a wall-bounded shear layer (i.e. a boundary layer). The boundary conditions used were those of Weisbrot's experiment (16), but the domain was kept two-dimensional because of memory and speed limitations on the CRAY X-MP 12 computer.

2. Code and Grid Information

The discretized analog of the two-dimensional Navier-Stokes equations that was used was the finite difference algorithm of MacCormack (17) as implemented by Shang (18). Shang's code was modified by removing the pressure damping subroutine and the turbulence model subroutine. Shang's code is second-order accurate in time and space (19:483). Consequently, the highest order error terms due to discretization are third order (dispersive). The code was run time-accurately with a Courant-Friedrichs-Lewy number of .8 to insure stability of the calculation.

The computational domain was 4.99 feet long and 1.64 feet wide. See Figure 5 for a view of a sparsely gridded version of the upper half of the grid. The domain had 947 streamwise points and 98 cross-stream points for a total of 92,806 grid points. The computational cells were kept as square as possible

in the mixing layer "cone," a region of densely packed cells whose upstream boundary was .05 feet wide and whose downstream boundary was .5 feet wide. Figures 6 and 7 show closeup views of cells near the centerline at the upstream and downstream boundaries, respectively. The cone had 38 points crosswise. Sixty additional points were placed outside (30 on each side) with a stretching routine that smoothly transitioned the spacing from the cone dense packing to a sparser spacing at the top and bottom boundaries.

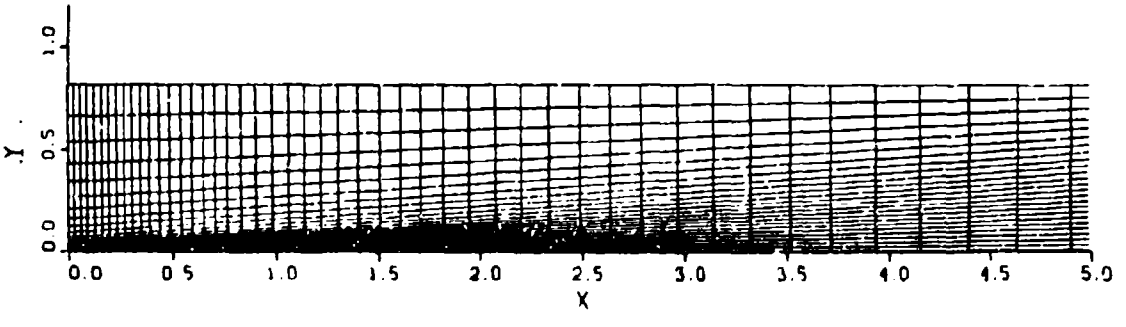

Figure 5, Upper Half of Grid (Not every line is shown)

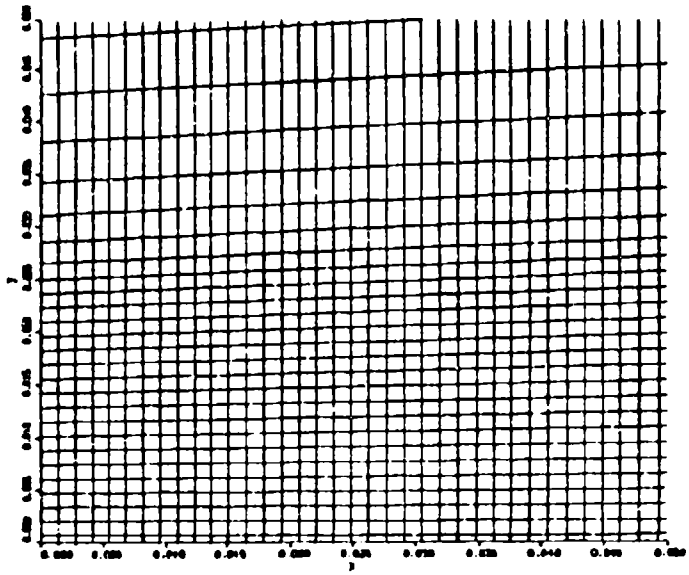

Figure 6, Grid Section at Upstream Boundary

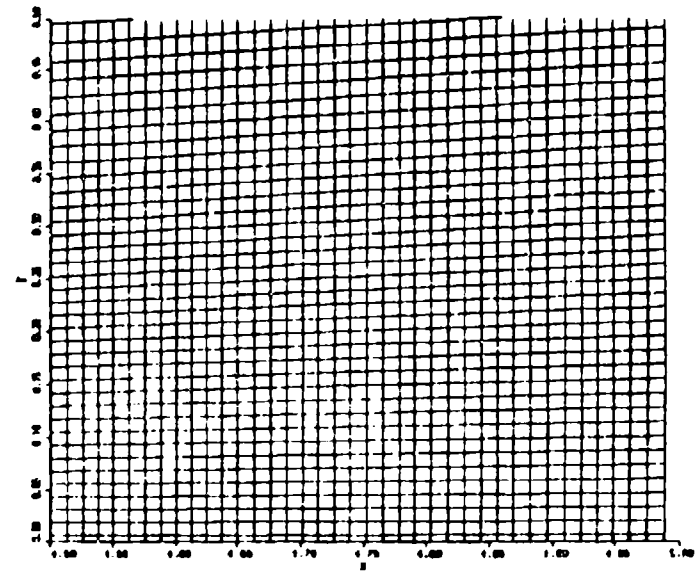

Figure 7, Grid Section at Downstream Boundary

3. Boundary Conditions

Figure 8 shows the boundary conditions for the computation. The flow speed for $x_2 > 0$ was 35.45 feet/sec, and the flow speed for $x_2 < 0$ was 21.27 feet/sec. These inflow conditions deviated slightly from Weisbrot's (32.808 feet/sec and 19.685 feet/sec) because of an input mistake. A 1/7th power law was applied to simulate both boundary layers coming off the splitter plate. The boundary layers were the same thickness, .025 feet. Initially, a steady-state upstream boundary condition was tried, but experience showed that some unsteadiness, even if only on the order of freestream turbulence (.1%), was required in order to create vortical structures in the shear layer. Davis and Moore (20); McInville, Gatski, and Hassan (21); and Grinstein, Oran, and Boris (22:209) also found it necessary to excite the flow at some point. While the present study did not explicity explore the sensitivity of shear layer roll-up to disturbance amplitude, in earlier work by the authors a simple sinusoidally oscillating u_2 component impressed on the steady state flow with amplitudes of .3% of free stream (high speed side of shear layer) was found to induce formation of structures in the shear layer. Davis and Moore (20) found that amplitudes as low as .2% would cause reasonably prompt roll-up of the shear layer. Below .2%, the distance from the front boundary to roll-up lengthened considerably. For the results presented here, u_2 was oscillated

at one percent of freestream at 44.5 Hz in order to simulate Weisbrot's experimental conditions (16). All computations started with uniform high speed flow for $x_2>0$ and uniform low speed flow for $x_2<0$ except for boundary layer profiles placed on either side of the channel center line.

The boundary conditions in Figure 8 worked adequately well as long as the flow which started at the upstream boundary did not convect asfar as the downstream boundary. This was the case for all results presented in this paper. One attempt to convect these upstream structures through the downstream boundary failed (the computation became unstable). Grinstein et al (22:207-209) reported success in overcoming this problem with a pressure extrapolation scheme to a downstream farfield. Davis and Moore (20) took a slightly different approach by transforming the downstream portion of the domain to infinity and then enforcing zero gradient conditions there. Either one of these schemes would likely solve the current downstream problem.

TOP

$$\rho u_1 = (\rho u)_\infty \qquad \frac{\partial(\rho u_2)}{\partial x_2} = 0$$

$$\rho e = \rho\left(c_v T_\infty + \frac{1}{2}(u_1^2 + u_2^2)\right) \quad \text{and} \quad \frac{\partial P}{\partial x_2} = 0 \text{ is approximated by}$$

$$\rho(K,98) = \rho(K,97)\left[e(K,97) - \frac{1}{2}(u_1(K,97)^2 + u_2(K,97)^2)\right]/c_v T_\infty$$

UPSTREAM

$\rho = \rho_\infty$

$\rho u_2 = .01(\rho u_\infty)\sin[44.5(2\Pi t)]$

$\rho e = (\rho e)_\infty$

$\rho u_1 = (\rho u)_\infty$ for $x_2 > 0$

$\rho u_1 = .6(\rho u)_\infty$ for $x_2 < 0$

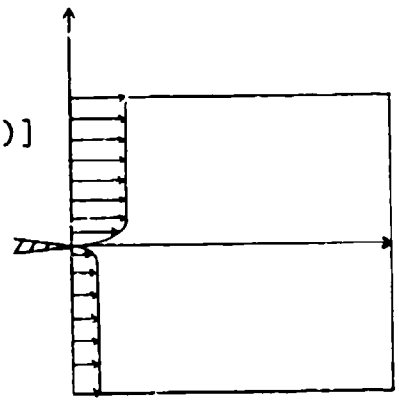

DOWNSTREAM

All

Streamwise

First-order

Gradients

Are Zero

BOTTOM

$$\rho u_1 = .6(\rho u)_\infty \qquad \frac{\partial(\rho u_2)}{\partial x_2} = 0$$

$$\rho e = \rho\left(c_v T_\infty + \frac{1}{2}(u_1^2 + u_2^2)\right) \quad \text{and} \quad \frac{\partial P}{\partial x_2} = 0 \text{ is approximated by}$$

$$\rho(K,1) = \rho(K,2)\left[e(K,2) - \frac{1}{2}(u_1(K,2)^2 + u_2(K,2)^2)\right]/c_v T_\infty$$

Figure 8, Boundary Conditions for the Computations

4. Computation Results

Figures 9 and 10 present "snapshots" of the vorticity fields for the two computations at an elapsed time of .1242 seconds from computation start. Solid lines denote positive vorticity; dashed lines denote negative vorticity. The vorticity fields are very similar. The upstream boundary emits positive vorticity (solid lines) and negative vorticity (dashed lines) corresponding to the two boundary layers. Both computations show waves growing as the fluid in the shear layer moves downstream. At a point a little over one foot from the upstream boundary, the laminar shear layer transitions to a turbulent shear layer as individual vortices roll up and interact with one another as they move downstream. This proves that the Shang code can predict laminar to turbulent transition in a low speed, two-dimensional free shear layer. To the authors' knowledge, it is the first time a compressible, Navier-Stokes code has demonstrated this capability. This is probably due in part to the punitive computational resources required. Each of the current computations required 200,000 iterations at a cost of 34 central processing unit hours on a Cray XMP-12. Nevertheless, the current work does establish that it is possible and presents one approach for computing the flow.

Although the current inflow conditions specified u_1 speeds slightly higher than that actually used in Weisbrot's experiment (16) and Figures 9 and 10 show vorticity most likely at a

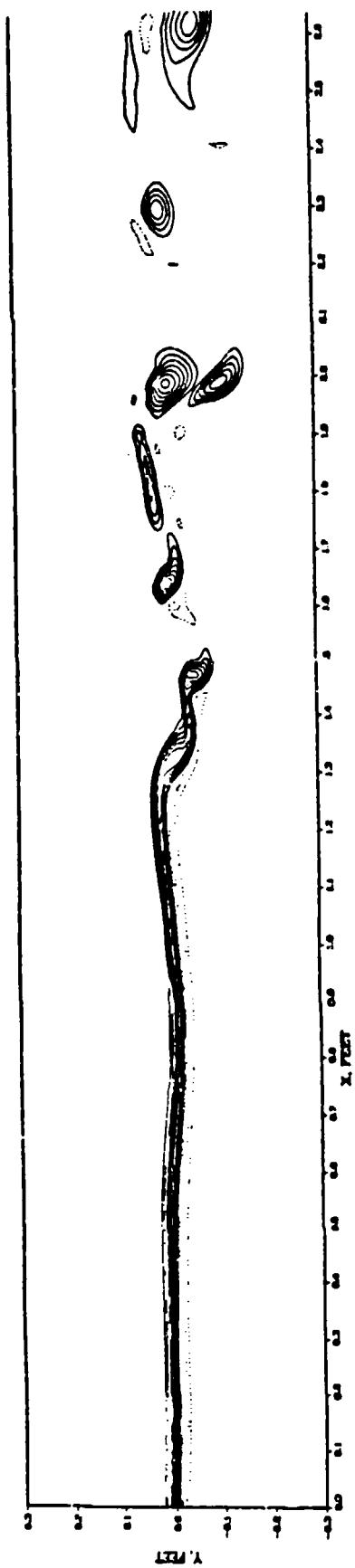

Figure 9, Vorticity Computed With Asymmetric Stress Tensor

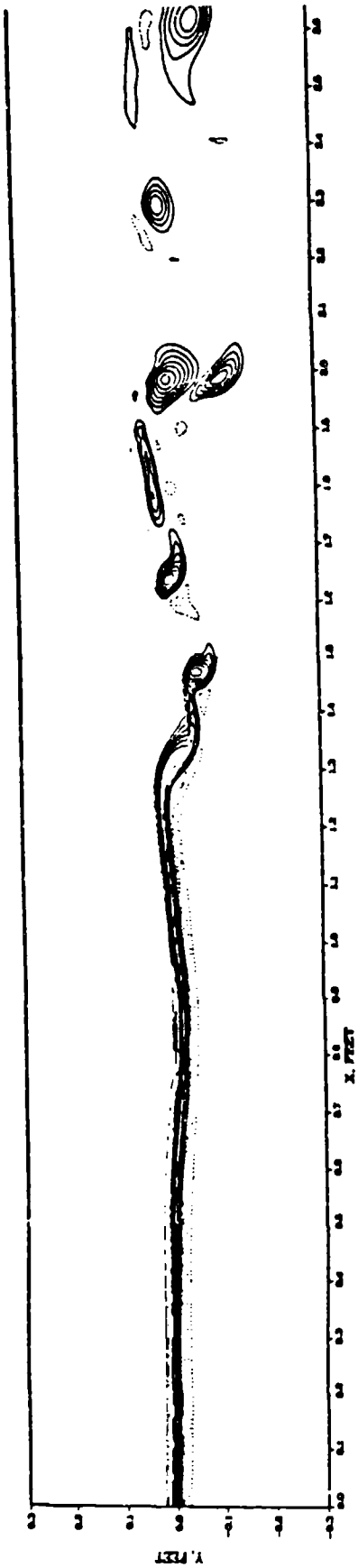

Figure 10, Vorticity Computed With Symmetric Stress Tensor

different phase of the upstream boundary excitation than that reported by Weisbrot, some similarities between computed and experimental results can be seen. Figure 11 shows vorticity contours which Weisbrot educed by sampling the flowfield at the same frequency as the splitter plate oscillation frequency. Two main features appear. Upstream, a vorticity zone appears as a layer tilted slightly downstream. Downstream, two vortical structures appear, one directly over the other. Similar structures can be seen in Figures 9 and 10. The two structures in the process of rolling up in the range of x_1 from 1.3 to 1.5 feet look like Weisbrot's tilting vorticity layer. The two vortices stacked on top of one another at x_1 of 2 feet look like the downstream stacked vortices in Figure 11.

The qualitative similarities aside, it is useful to study where in the flowfield the eigenvalue of the $\mu = -\nu$ stress tensor becomes complex so as to aid in understanding differences in the computed results. Figure 12 shows the regions of imaginary eigenvalue as given by equation 18. Curiously, only some regions of the laminar shear layer have imaginary stress eigenvalues. One such region is the wave that extends from x_1 of .5 feet to .8 feet, and, if one looks downstream about .6 feet (the distance corresponding to the upstream excitation

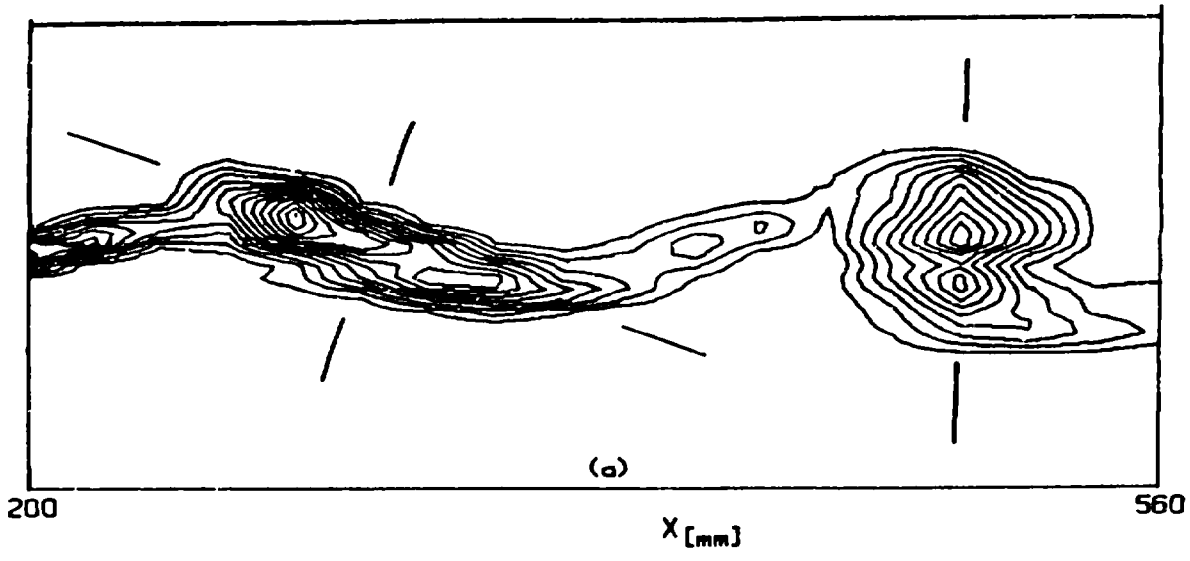

Figure 11, Educed Vortical Structures (Weisbrot, reference 16)

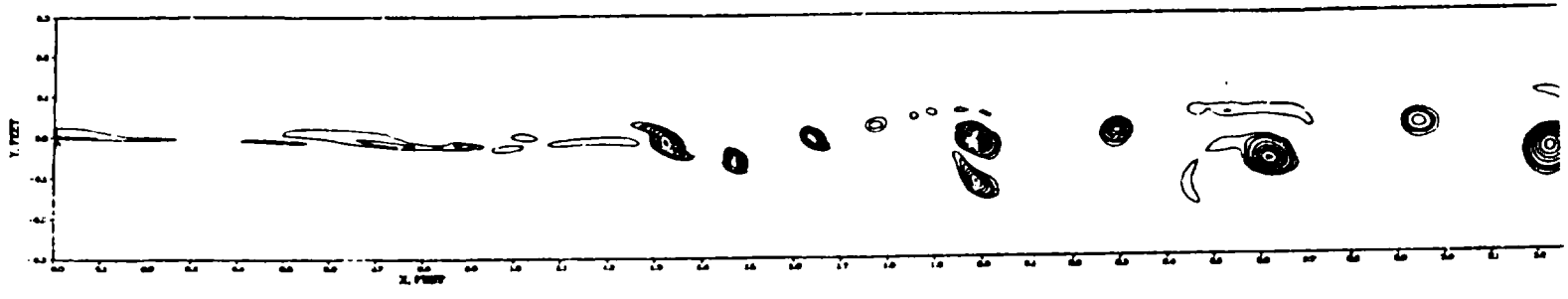

Figure 12, Imaginary Eigenvalue Field

frequency and the mean shear layer speed), one sees a shape that looks somewhat like a galaxy. This "galaxy" is apparently what the wave will become. The imaginary eigenvalue condition appears to be able to identify a vortical structure while it is still just a wave presumably because both the wave and the vortical structure have a common characteristic described by the iamginary eigenvalue condition. The vorticity contours in Figures 9 and 10 make no such distinction. However, downstream of the laminar shear layer rollup, the imaginary eigenvalue contours in Figure 12 look very similar to the vorticity field contours in Figures 9 and 10.

Because the wave and the galaxy appear to be two characteristic regions of complex stress eigenvalues, they will be analyzed in more detail for differences between the two computations. For the sake of completeness, the vortex at x_1 of 1.47 feet (just downstream of the galaxy) will be included in the comparison. These regions of imaginary stress eigenvalue (the wave, galaxy, and vortex) are likely regions to look for differences between the computations, because the complex nature of the $\mu = -\nu$ principal stresses in these regions might be expected to induce the solution to behave differently due to the fact that the symmetric stress tensor does not possess the property of conditional imaginary eigenvalues.

Figures 13, 14, and 15 present labeled vorticity contour plots for the wave, galaxy, and vortex respectively. Peak vorticity is seen in the wave. It is about 1100 feet/sec/foot.

In the galaxy and vortex, peak vorticity is about 700 feet/sec/foot.

Figures 16, 17, and 18 present labeled vorticity difference plots for the wave, galaxy, and vortex respectively. Positive values mean that the symmetric stress tensor computation predicted vorticity that was larger than that predicted by the $\mu = -\nu$ stress tensor computation. The wave (Figure 16) shows extremely small differences, only as high as .8 feet/sec/foot. The galaxy shows somewhat larger differences, some as high as 7 feet/sec/foot. Most of the difference is centered in the clump at $x_1 = 1.35$ feet and $x_2 = -.05$ feet. The vortex (Figure 18) also shows peak differences of about 7 feet/sec/foot. The differences are organized into four zones and alternate between positive and negative as one moves around the vortex. In fact, four similar zones can be seen to be forming in the galaxy (Figure 17). What meaning the four zone pattern might have, if any, is unclear. In any event, given that peak vorticity in the galaxy and vortex is about 700 feet/sec/foot, peak differences in vorticity of about 7 feet/sec/foot only amount to one percent of the peak vorticity. Consequently, when using vorticity as the ruler for measuring the differences between the computations, one must conclude that the effect of the $\mu = -\nu$ stress tensor on the computation of a low speed, two-dimensional free shear layer is minimal when compared to the computation of the same shear layer using the $\nu = 0$ stress tensor.

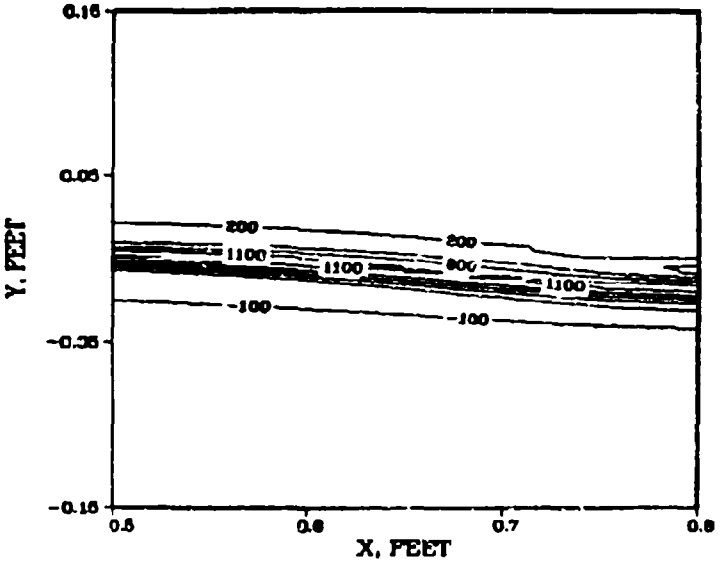

Figure 13, Vorticity (ν = 0, Wave)

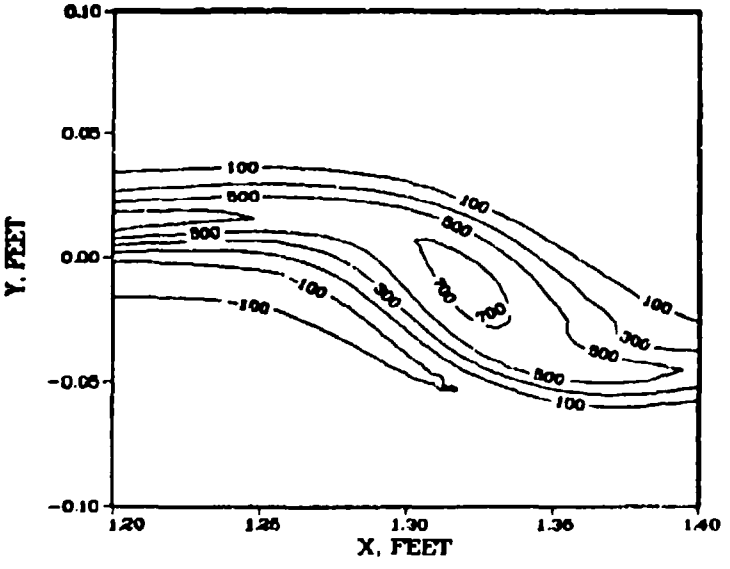

Figure 14, Vorticity (ν = 0, Galaxy)

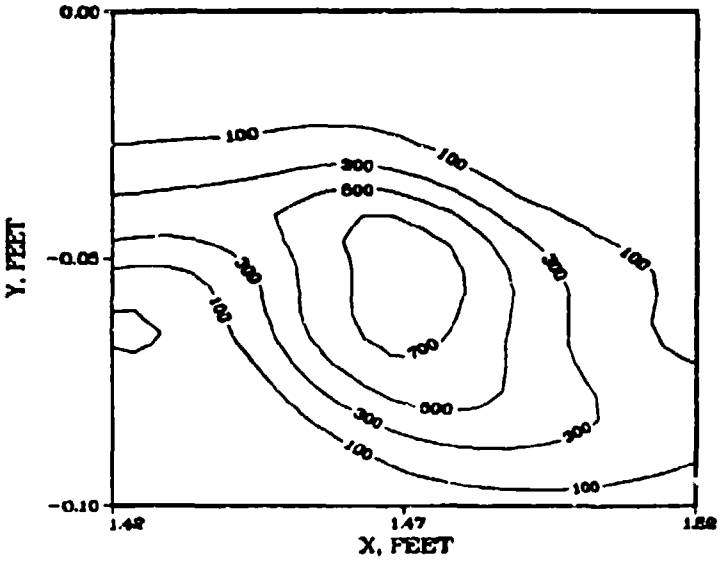

Figure 15, Vorticity (ν = 0, Vortex)

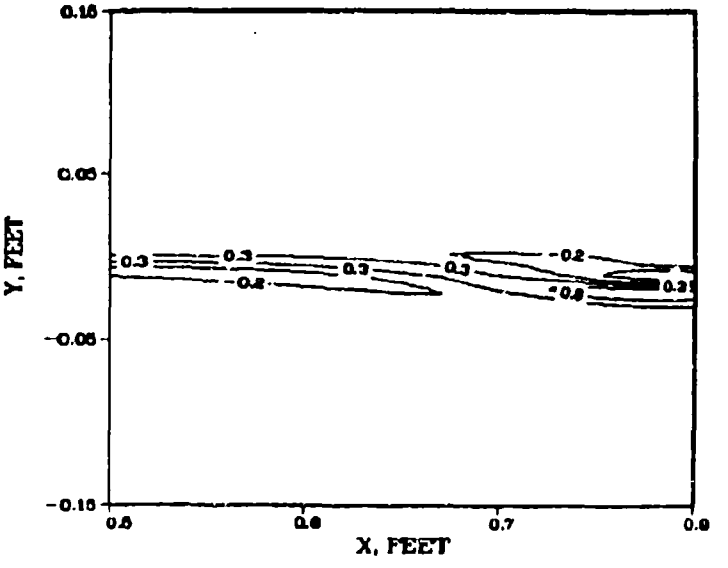

Figure 16, Vorticity Difference (Wave)

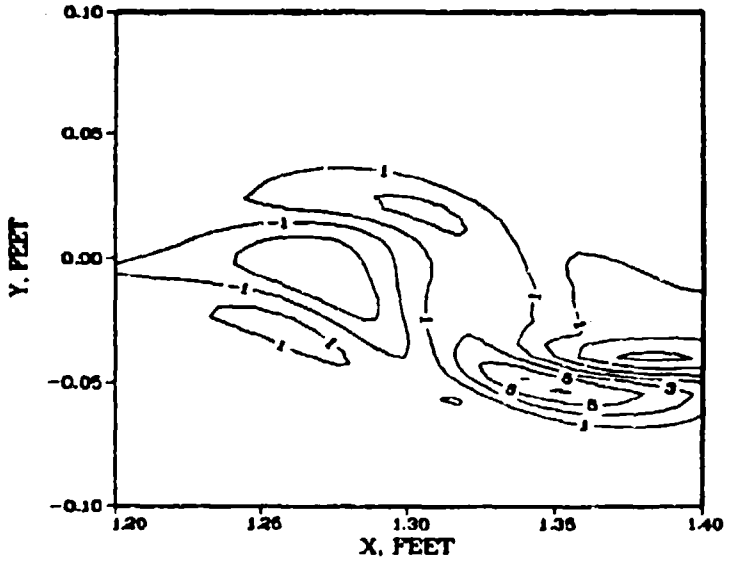

Figure 17, Vorticity Difference (Galaxy)

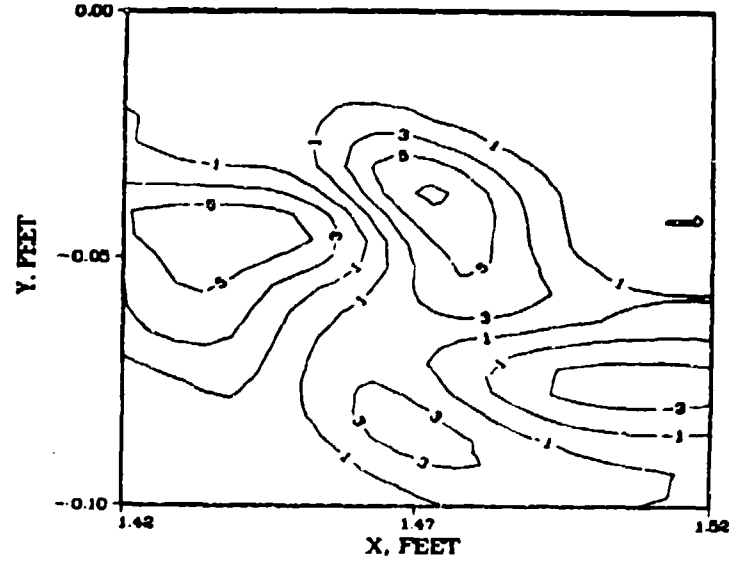

Figure 18, Vorticity Difference (Vortex)

Although differences between the computations do appear, characterizing the development of the differences seems difficult. Perhaps the $\mu = -\nu$ complex principal stresses cause a dispersion or phase shift effect as suggested by the simple one-dimensional scalar convection equation presented earlier in this paper. In any event, the present results do show small differences in the computed flowfields.

SECTION IV

CONCLUSION

The study concludes that an asymmetric stress tensor influenced by vorticity contains advantages over the classic Stokesian approach. By including the effects of all three of the basic motions about a point in a fluid, a more intuitively satisfying prediction of stress on a small fluid cube is obtained. The principal stresses of this new vorticity-influenced stress tensor become complex when a shear layer turns away from the higher speed flow such as in a perturbed shear layer or in a vortex. Although the classic theory might raise objections to the idea of an asymmetric stress tensor, these objections appear difficult to support. Computer experiments demonstrate that a two-dimensional, compressible Navier-Stokes code (the Shang code) can predict the transition from laminar to turbulent flow, but the symmetric and asymmetric stress tensors only change predicted vorticity by a maximum of approximately one percent in the vicinity of the two vortical structures examined.

SECTION V

RECOMMENDATIONS

1. Change the downstream boundary conditions to permit flux of upstream disturbances. Then, after the computation has run long enough to develop the flow in the entire computational domain, run the computation long enough to obtain reliable mean and spectral velocity data for comparison with Weisbrot's experimental data (16).

2. Explore the sensitivity of grid density on the solution. It would be helpful to know whether fewer grid points would yield an acceptable answer. This would reduce computation costs for future users as long as some rules of thumb could be established.

3. Run the same computation in an Euler mode and compare with experimental data. This would help establish the practicality of predicting shear layer mixing without having to resort to the extra expense of computing viscous terms.

4. When a more powerful computer becomes available, repeat the computation with a three-dimensional Navier-Stokes code to establish what benefits the extra dimension gives. Vortical structure interaction would probably not remain two-dimensional

for long in a real shear layer. A three-dimensional computation would help establish guidelines for the limits of the utility of two-dimensional calculations.

5. Develop a generic, robust, unsteady boundary condition for use upstream or on the surface of a vehicle. Perhaps such a boundary condition could excite a range of frequencies with continually varying phase. The frequency and phase content of disturbances in the flow appear very important for predicting the transition from laminar to turbulent flow.

ACKNOWLEDGEMENTS

The first author (CHB) would like to thank the second author (WZS) for proposing the idea that an asymmetric stress tensor could play a factor in turbulent flow.

REFERENCES

1. Stokes, G. G.: "On the Theories of Internal Friction of Fluids in Motion", Trans. Cambr. Phil. Soc. 8, 287-305 (1845).

2. Schlichting, H.: Boundary Layer Theory, (7th ed) McGraw-Hill, New York (1979).

3. Morkovin, M. V.: Guide to Experiments on Instability and Laminar-Turbulent Transition in Shear Layers, Dept. of Mech. and Aerospace Engineering, Illinois Institute of Technology, Chicago, Illinois (1985).

4. Batchelor, G. K.: An Introduction to Fluid Dynamics, Cambridge University Press, New York (1967).

5. Aris, Rutherford: Vectors, Tensors, and the Basic Equations of Fluid Mechanics, Prentice-Hall; Englewood Cliffs, N.J. (1962).

6. White, F. M.: Viscous Fluid Flow, McGraw-Hill, New York (1974).

7. Thompson, P. A.: Compressible-Fluid Dynamics, McGraw-Hill, New York (1972).

8. Karim, S. M. and Rosenhead, L.: "The Second Coefficient of Viscosity of Liquids and Gases," Reviews of Modern Physics, Vol. 24, No. 2, pp. 108-116, April 1952.

9. Rosenhead, L. (editor): "A Discussion On the First and Second Viscosities of Fluids," Proc. R. Soc. Lond. Ser. A, Vol. 226, pp. 1-69, 1954.

10. Truesdell, "The Mechanical Foundations of Elasticity and Fluid Dynamics," Journal of Rational Mechanics and Analysis, Vol. 1 (1952).

11. Reynolds, O.: "An Experimental Investigation of the Circumstances Which Determine Whether the Motion of Water Shall Be Direct or Sinuous, and of the Law of Resistance in Parallel Channels," Phil. Trans. Roy. Soc. 174, 935-982 (1883).

12. Van Driest, E. R. and Blumer, C. B.: "Boundary Layer Transition: Freestream Turbulence and Pressure Gradient Effects," AIAA J., Vol 1, pp. 1303-1306 (1963).

13. Dimotakis, P. E.: personal conversation at California Institute of Technology, Oct 1984.

14. Fasel, H. F.: "Stability and Transition Investigations Using the Navier-Stokes Equations," Twelfth Symposium on Naval Hydrodynamics, Washington, D. C. (June 5-9, 1978).

15. Evans, D. J. and Hoover, W. G., "Flows Far From Equilibrium via Molecular Dynamics," Annual Review of Fluid Mechanics, Palo Alto, California, Vol. 18, 1986.

16. Weisbrot, I.: "A Highly Excited Turbulent Mixing Layer," AFOSR Report AE 84-2, Nov 1984.

17. MacCormack, R. W.: "The Effect of Viscosity in Hypervelocity Impact Cratering," AIAA Paper 69-354, 1969.

18. Visbal, M.R. and Shang, J.S.: "A Comparative Study Between an Implicit and Explicit Algorithm for Transonic Airfoils," AIAA Paper 85-0480, 1985.

19. Anderson, D. A.; Tannehill, J. C.; and Pletcher, R. H.; Computational Fluid Dynamics and Heat Transfer; McGraw-Hill, New York, 1984.

20. Davis, R.W. and Moore, E.F.: "A Numerical Study of Vortex Merging in Mixing Layers," Phys. Fluids 28 (6), June 1985.

21. McInville, R.M.; Gatski, T.B.; and Hassan, H.A.: "Analysis of Large Vortical Structures in Shear Layers," AIAA Paper 84-0349, 1984.

22. Grinstein, F. F.; Oran, E. S.; and Boris, J. P.; "Numerical Simulations of Asymmetric Mixing in Planar Shear Flows;" J. Fluid Mech.; Vol. 165, 1986, pp. 201-220.

U.S.Government Printing Office: 1987 — 748-061/60827